Chemical Physics Letters 683 (2017) 140–144

Contents lists available at ScienceDirect

Chemical Physics Letters

journal homepage: www.elsevier.com/locate/cplett

Research paper

# Investigation of charge separation in particulate oxysulfide and oxynitride photoelectrodes by surface photovoltage spectroscopy

Masanori Kodera [a], Jiarui Wang [b], Benjamin A. Nail [b], Jingyuan Liu [a], Haruki Urabe [a], Takashi Hisatomi [a], Masao Katayama [a], Tsutomu Minegishi [a], Frank E. Osterloh [b,*], Kazunari Domen [a,*]

[a] Department of Chemical System Engineering, School of Engineering, The University of Tokyo, 7-3-1 Hongo, Bunkyo-ku, Tokyo 113-8656, Japan
[b] Department of Chemistry, University of California, Davis, One Shields Avenue, Davis, CA 95616, United States

ARTICLE INFO

*Article history:*
Received 29 December 2016
In final form 4 March 2017
Available online 6 March 2017

*Keywords:*
Photoelectrochemical water splitting
Surface photovoltage spectroscopy
Interface
Particle transfer method

ABSTRACT

Surface photovoltage spectroscopy (SPS) was applied to the analysis of particulate $La_5Ti_2CuS_5O_7$ and $SrNbO_2N$ photoelectrodes fabricated by a particle transfer method, as a means of assessing charge separation under illumination. The critical roles of the back contact metals and cocatalyst in generating charge separation and defining various photoelectrochemical properties were confirmed. The results suggests that SPS in conjunction with particle transfer technology potentially allows the identification of the most beneficial photoelectrode components for photoelectrochemical water splitting.



## 1. Introduction

Oxysulfide and oxynitride semiconductors have received much attention as potential photocatalysts for renewable hydrogen production via sunlight-driven water splitting, owing to their ability to absorb visible light [1]. As an example, $La_5Ti_2CuS_5O_7$, having an absorption edge at 650 nm, works as either a photoanode or a photocathode in conjunction with Ti or Au back electrodes, respectively [2,3]. Series-connected $La_5Ti_2CuS_5O_7$ photoanodes and photocathodes have been reported to allow photoelectrochemical (PEC) water splitting without the application of an external bias under visible light illumination. $SrNbO_2N$ absorbs light up to 690 nm and has been shown to function as a photoanode for PEC water oxidation [4]. In addition, modification with cocatalysts such as CoPi effectively improves the PEC properties of $SrNbO_2N$ photoanodes [5]. In these photoelectrode systems, charge separation at the interfaces between particulate semiconductors and back electrodes or cocatalysts evidently affects the PEC properties. Indeed, charge transfer processes are central to the activation of oxysulfide and oxynitride photoelectrodes, based on their narrow band gaps and minimal driving forces for the water splitting reaction.

Surface photovoltage spectroscopy (SPS) is a powerful tool for the analysis of charge separation processes in semiconducting devices such as solar cells, photocatalysts and photoelectrodes [6–8]. In this technique, the surface photovoltage is measured under various atmospheres, including under vacuum. During irradiation of the sample by monochromatic light, changes in the surface photovoltage resulting from charge separation can be monitored to obtain a spectrum [9–11]. Charge separation properties can be evaluated as the sign and the magnitude of the SPS signal even if photocurrent or product is not observable in non-biased conditions. When applying this method to the study of particulate photocatalysts as potential photoelectrodes, it is vital that these materials have sufficient electrical contact with a back electrode.

Recently, our group reported particle transfer as a novel method for the fabrication of electrodes based on particulate photocatalysts [12]. In this technique, only a few layers of photocatalyst particles are rigidly embedded into a metal film. Therefore, composites of various particulate photocatalysts and metal films exhibiting low contact resistances can be obtained reproducibly. This is preferable with regard to SPS because the effects of variations in the film thickness and contact resistance between semiconducting particles and the back electrode can be reduced. In the present work, the charge separation characteristics of highly-crystalline particulate $La_5Ti_2CuS_5O_7$ and $SrNbO_2N$ photoelectrodes incorporating different back electrodes fabricated by the particle transfer method were studied by SPS. Our results indicate the significant effects of the semiconductor-back contact interface and the semiconductor-cocatalyst interface on the spatial charge separation and the PEC properties.

* Corresponding author.
*E-mail address:* domen@chemsys.t.u-tokyo.ac.jp (K. Domen).

http://dx.doi.org/10.1016/j.cplett.2017.03.012
0009-2614/

## 2. Experimental

Sc-doped $La_5Ti_2CuS_5O_7$ was synthesized by a solid state reaction in sealed evacuated tubes [2]. $SrNbO_2N$ was obtained by nitriding $Sr_2Nb_2O_7$ synthesized using a flux method [5]. Photoelectrodes composed of Sc-doped $La_5Ti_2CuS_5O_7$ or $SrNbO_2N$ were fabricated via a particle transfer method [12]. The photocatalyst powder was suspended in 2-propanol and this suspension was dropped onto a glass plate, then dried at room temperature. In the case of the Sc-doped $La_5Ti_2CuS_5O_7$ powder, a Ti or Au (>2 μm) metal layer was deposited by radio-frequency (RF) magnetron sputtering or thermal evaporation, respectively. For the $SrNbO_2N$ powder, a layer of either Nb or Au (300–400 nm in thickness) was deposited by RF magnetron sputtering or thermal evaporation, respectively. A thick Ti layer (>5 μm) was additionally deposited by RF magnetron sputtering to ensure the continuity and mechanical strength of the film. The obtained films incorporating the photocatalyst powder were transferred to a second glass plate using double-side tape and ultrasonicated in water to remove particles that were not firmly held by the metal film.

Current-potential curves were acquired using a three-electrode configuration under intermittent illumination with simulated AM 1.5G sunlight (San'ei Denki, XES-40S2-CE). A Pt wire and an Ag/AgCl electrode were used as the counter and reference electrodes, respectively. The potential was swept at a scan rate of 10 mV $s^{-1}$ with a potentiostat (HSV-110, Hokuto Denko). The potentials were calculated using the equation $E\ [V_{RHE}] = E_0\ [V_{Ag/AgCl}] + 0.199 + 0.0591 \times pH$. For $La_5Ti_2CuS_5O_7$ photoelectrodes with Au and Ti electrodes, the electrolyte used was a 0.1 M aqueous sodium sulfate solution adjusted to a pH of 10 by NaOH addition [2,3]. In the case of $SrNbO_2N$ photoanodes, the electrolyte was a 0.2 M aqueous sodium phosphate solution adjusted to a pH of 13 by NaOH addition. In some cases, a CoPi cocatalyst was deposited by electrodeposition at 1.7 V vs. reversible hydrogen electrode (RHE) for 200 s [13].

SPS data were acquired using a vibrating gold Kelvin probe (Delta PHI Besocke) mounted in a vacuum chamber of our own design ($< 1 \times 10^{-4}$ mbar). Monochromatic light was provided from a 150 W Xe lamp filtered through a grating monochromator (Oriel Cornerstone 130). Contact potential difference (CPD) spectra were corrected for drift effects by subtracting a dark scan. In some experiments, the samples were wetted with methanol and then dried in an oven at 323 K prior to acquiring spectra.

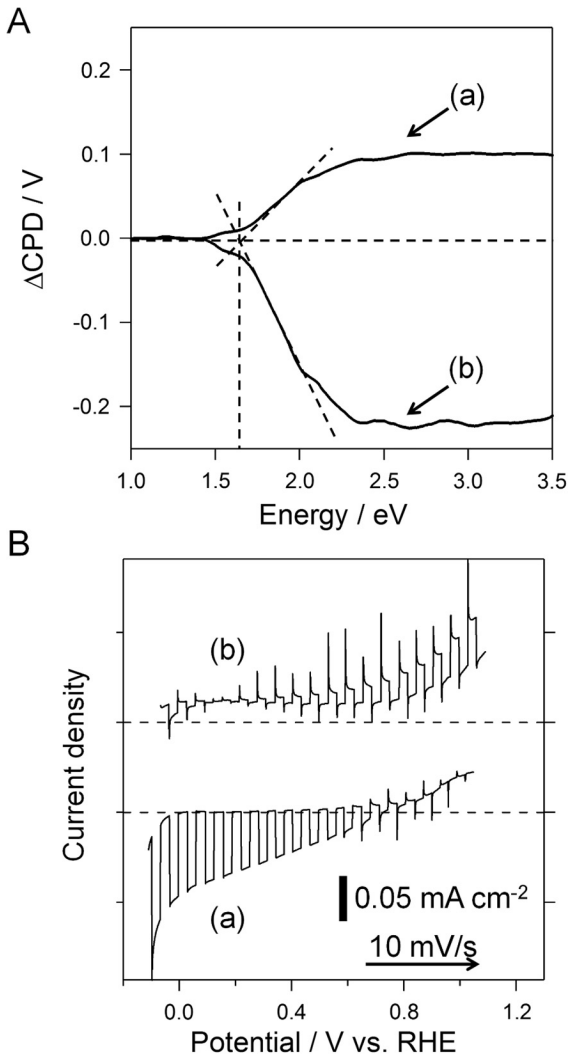


**Fig. 1.** (A) Surface photovoltage spectra and (B) current-potential curves for Sc-doped $La_5Ti_2CuS_5O_7$ photoelectrodes with (a) Au and (b) Ti back electrodes. PEC measurement were performed under intermittent simulated sunlight (AM 1.5G) in an aqueous 0.1 M $Na_2SO_4$ solution adjusted to pH 10 with NaOH.

## 3. Results and discussion

### 3.1. $La_5Ti_2CuS_5O_7$ photoelectrodes

Fig. S1 presents an XRD pattern and a diffuse reflectance spectrum for Sc-doped $La_5Ti_2CuS_5O_7$ powder and an SEM image of a Sc-doped $La_5Ti_2CuS_5O_7$/Au electrode. The Sc-doped $La_5Ti_2CuS_5O_7$ had an absorption edge of 650 nm and was evidently composed of columnar particles. As shown in Fig. 1A, positive and negative CPD signals were observed when Au and Ti were employed as the back electrodes, respectively. This indicates that holes migrated from the Sc-doped $La_5Ti_2CuS_5O_7$ to the back contact metal while electrons were accumulated on the surface for the Sc-doped $La_5Ti_2CuS_5O_7$/Au electrode and vice versa for the Sc-doped $La_5Ti_2CuS_5O_7$/Ti electrode (see Fig. S2). The strong dependence on the substrate suggests that the photovoltage creation in both cases is due to carrier separation at the semiconductor/back electrode interface. This result is consistent with photoelectrochemical properties presented in Fig. 1B in which $La_5Ti_2CuS_5O_7$/Au and $La_5Ti_2CuS_5O_7$/Ti electrodes functioned as photocathodes and photoanodes, respectively. Our previous work also demonstrates that charge separation at the solid/solid junction between the $La_5Ti_2CuS_5O_7$ particles and the back electrode determines the PEC properties [3]. The onset energy for the CPD signals was 1.6 eV for both Sc-doped $La_5Ti_2CuS_5O_7$/Au and Sc-doped $La_5Ti_2CuS_5O_7$/Ti electrodes. This value is less than the optical band gap energy of 1.9 eV, presumably because of excitation involving surface states of intermediate energy.

An energy band diagram for Sc-doped $La_5Ti_2CuS_5O_7$ and the work functions for Ti (4.33 eV) and Au (5.4 eV) are presented in Fig. 2A [14,15]. We previously reported that the valence band maximum for $La_5Ti_2CuS_5O_7$ was −5.7 V vs. vacuum [3]. Because negative and positive CPD signals were observed, the Fermi level of Sc-doped $La_5Ti_2CuS_5O_7$ is considered to be between the work functions of Ti and Au so that a depletion and accumulation layer can be formed when Sc-doped $La_5Ti_2CuS_5O_7$ is in contact with Ti and Au (Fig. 2B), respectively. Accordingly, the bands bend up or down, as shown in the figure. In fact, the Fermi levels for undoped and Ga-doped $La_5Ti_2CuS_5O_7$ were recently reported to be 0.95 and 0.6 V more negative than the valence band maximum (−4.75 and −5.1 V vs. vacuum), respectively [16]. It is reasonable to assume that Sc-doped $La_5Ti_2CuS_5O_7$ has a similar Fermi level. In the case of the $La_5Ti_2CuS_5O_7$/Ti electrode, downward band-bending

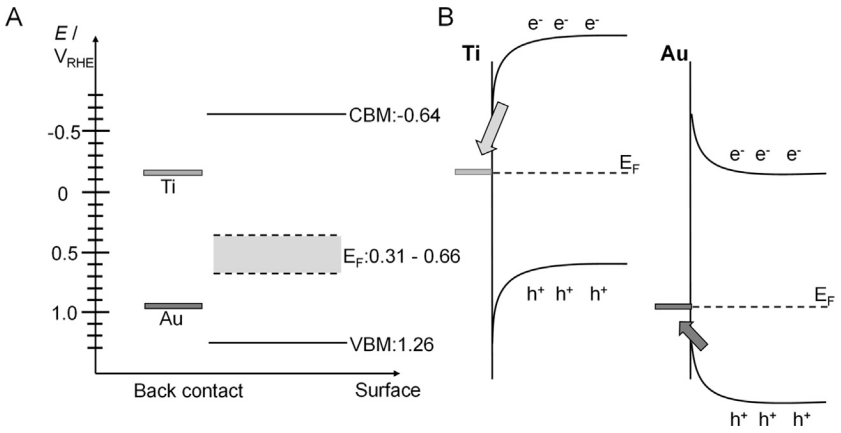


**Fig. 2.** (A) Energy diagram for Sc-doped $La_5Ti_2CuS_5O_7$ photoelectrodes with different back electrodes. The work functions for metals are from the literatures [14,15]. The potentials were calculated using the equation $E\ [V_{RHE}] = -E_0\ [V_{vacuum}] - 4.44\ [V]$. (B) Expected band diagram for Sc-doped $La_5Ti_2CuS_5O_7$/Ti and Sc-doped $La_5Ti_2CuS_5O_7$/Au interfaces.

prevents the migration of holes from the $La_5Ti_2CuS_5O_7$ to the Ti layer, while promoting migration of electrons to the Ti layer. In contrast, the $La_5Ti_2CuS_5O_7$/Au electrode rectifies the flow of photoexcited carriers in the opposite manner because of the upward band-bending. Unlike a typical particulate oxynitride and oxysulfide semiconductor, $La_5Ti_2CuS_5O_7$ exhibits long carrier lifetimes and diffusion lengths up to the micrometer range [17–19]. Excited holes and electrons can therefore migrate over the span of the Sc-doped $La_5Ti_2CuS_5O_7$ particles and consequently may be trapped at surface states. As a result, electrons and holes are spatially separated, and definite negative and positive CPD signals are experimentally observed for $La_5Ti_2CuS_5O_7$/Ti and $La_5Ti_2CuS_5O_7$/Au electrodes, respectively. Thus, SPS has been shown to clearly differentiate the PEC properties of Sc-doped $La_5Ti_2CuS_5O_7$ working as both a photoanode and a photocathode depending on the back electrode material.

### 3.2. $SrNbO_2N$ photoanodes

An XRD pattern and a diffuse reflectance spectrum obtained from the synthesized $SrNbO_2N$ powder and SEM images of $SrNbO_2N$/Nb electrodes are shown in Fig. S3. From these data, it is evident that well-crystallized $SrNbO_2N$ particles without impurity phases were synthesized. The secondary particles of $SrNbO_2N$ were several micrometers in size and composed of bundles of columnar grains. The band gap energy for $SrNbO_2N$ was estimated to be 1.85 eV from the diffuse reflectance spectrum, and this value is consistent with previous reports [4,5]. The SEM images show that several layers of these $SrNbO_2N$ secondary particles were embedded into the metal layer.

Fig. 3 presents SPS results for $SrNbO_2N$/Nb and $SrNbO_2N$/Au electrodes with and without the CoPi cocatalyst, along with the corresponding current-potential curves acquired under chopped simulated sunlight irradiation. Negative CPD signals were observed for both $SrNbO_2N$/Nb and $SrNbO_2N$/Au electrodes, indicating that electrons migrated from the $SrNbO_2N$ toward the back contact metals while holes were accumulated on the surface (see Fig. S2). This is consistent with the finding that the $SrNbO_2N$ electrodes exhibited a photoanodic current in the electrochemical experiments (Fig. 3C). The onset energy for the negative CPD signal was 1.64 eV. This value is approximately 0.2 eV smaller than the optical band gap energy and is attributable to the excitation of carriers in mid-gap states, such as impurity levels and surface states, to the conduction band [20,21]. However, the magnitude of the CPD signal was weak and barely observable when it was compared with a metal electrode as a control, suggesting low efficiencies of charge separation at the $SrNbO_2N$/metal interface. After loading with the CoPi cocatalyst, the intensity of the negative CPD signals was significantly enhanced. The CPD signal was also increased following treatment with methanol acting as a hole trapping reagent, as shown in Fig. S4. These results indicate that the CoPi cocatalyst had the ability to extract holes from $SrNbO_2N$ and thereby promote charge separation at the $SrNbO_2N$/CoPi interface in addition to reducing the kinetic overpotential for the oxygen evolution reaction. As can be seen from Fig. 3C, the photocurrent densities for the unmodified $SrNbO_2N$ photoelectrodes were all lower than 0.1 mA $cm^{-2}$ at 1.2 V vs. RHE regardless of the metal (Nb or Au) at the back contact. However, the photocurrent was increased by loading CoPi. The increment in the photocurrent upon CoPi loading was more significant for the $SrNbO_2N$/Nb electrode than for the $SrNbO_2N$/Au electrode.

As shown in the energy diagrams (Fig. 4), the work functions for Nb and Au are 4.3 and 5.4 eV, respectively [14,15]. In addition, the Fermi level for $SrNbO_2N$ was determined to be −0.1 V vs. RHE by a Mott-Schottky analysis (Fig. S5A). Therefore, we believe that an ohmic contact was formed at the interface between the $SrNbO_2N$ particles and the Nb back electrode and thus the energy barrier for electron injection into Nb was very small. In contrast, the $SrNbO_2N$/Au electrodes form a Schottky junction that prevents electron migration from $SrNbO_2N$ particles and the Au layer at the interface. As a result, $SrNbO_2N$/Nb outperformed $SrNbO_2N$/Au as a photoanode. This tendency is in accordance with particulate and single-crystalline $SrTiO_3$ photoanodes [22], where the use of low work function metals as back electrodes produced more efficient $SrTiO_3$ photoanodes. Interestingly, the enhancement of the CPD signal by CoPi modification was more pronounced for the $SrNbO_2N$/Au than for the $SrNbO_2N$/Nb although the enhancement of the photoanodic current was greater for the latter. The same tendency was observed for the case of the methanol treatment (Fig. S4). Therefore, the difference of these two photoanodes is thought to stem from the interface of $SrNbO_2N$ particles and the back electrode material. Presumably, a large density of interfacial states causes trapping of electrons near the surface of $SrNbO_2N$ facing to the Au electrode. Although further investigations shall be necessary to discuss the nature of such interfacial states and correlate the intensity of SPS signals with the photoelectrochemical properties of $SrNbO_2N$ quantitatively, SPS hints important roles of the back electrode material in charge separation and trapping

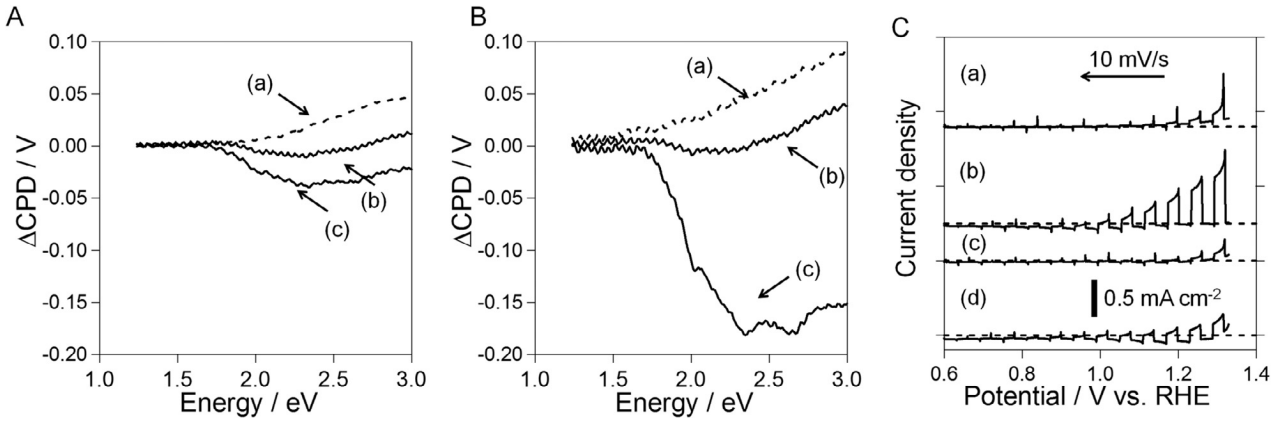


**Fig. 3.** Surface photovoltage spectra of (A) $SrNbO_2N$/Nb and (B) $SrNbO_2N$/Au photoelectrodes. (a) spectra of Nb or Au substrates as a reference, and (b, c) $SrNbO_2N$ electrodes (b) without and (c) with CoPi modification. (C) Current-potential curves for (a) $SrNbO_2N$/Nb, (b) CoPi/$SrNbO_2N$/Nb, (c) $SrNbO_2N$/Au, and (d) CoPi/$SrNbO_2N$/Au electrodes acquired under intermittent simulated sunlight (AM 1.5G) in an aqueous 0.2 M $Na_3PO_4$ solution adjusted to pH 13 with NaOH.

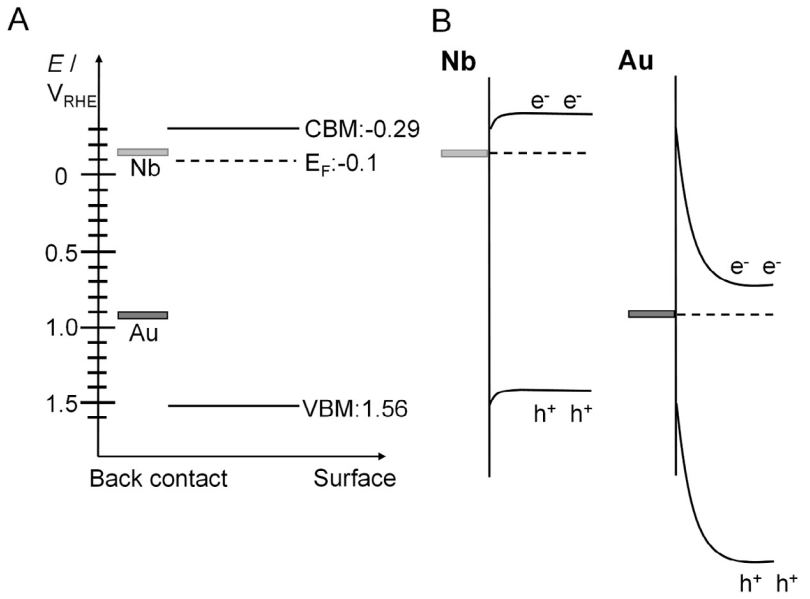


**Fig. 4.** (A) Energy diagram for $SrNbO_2N$ with different back electrodes. The work functions for the metals are from the literatures [14,15]. The potentials were calculated using the equation $E\ [V_{RHE}] = -E_0\ [V_{vacuum}] - 4.44$ [V]. (B) Expected band diagrams for $SrNbO_2N$/Nb and $SrNbO_2N$/Au interfaces.

processes owing to its ability to evaluate charge migration at the $SrNbO_2N$/back electrode and $SrNbO_2N$/cocatalyst interfaces separately.

## 4. Summary

The CPD signals for particulate semiconductor electrodes prepared by particle transfer were shown to be affected by both the semiconductor-back electrode interface and the semiconductor surface. In the case of $La_5Ti_2CuS_5O_7$, the application of different back electrode materials affected the charge separation and thereby the PEC properties of the materials. In the case of $SrNbO_2N$ electrodes, the negative CPD signals were enhanced upon loading with a CoPi cocatalyst and treatment with methanol because holes are trapped more efficiently on the surface. This effect is thought to contribute in part to the higher photocurrent. The use of high work function Au instead of Nb as the back electrode was found to enhance the negative CPD signals. However, this did not increase the photocurrent because of formation of a Schottky type contact.

SPS coupled with particle transfer technology allows to study charge separation at the interfaces of semiconductor/back electrode and semiconductor/cocatalyst separately in principle for any material combinations, including those that would be unstable in aqueous solution during photoelectrochemical measurements, taking unideal factors characteristic of particulate semiconductors such as surface trap states created during the sample preparation processes into account. In reality, the presence of surface states affects the properties of junction formed at solid/solid interfaces. Therefore, this method experimentally evaluating charge separation is potentially a powerful means of identifying desirable back electrode and cocatalyst materials as key components of particulate semiconductor photoelectrodes for more efficient PEC water splitting.

## Acknowledgements

This work was financially supported by Grants-in-Aid for Scientific Research (A) (No. 16H02417) and for Young Scientists (A) (No. 15H05494) from the Japan Society for the Promotion of Science

(JSPS). The present research was also supported in part through the Leading Graduate Schools Program, 'Global Leader Program for Social Design and Management,' of the Ministry of Education, Culture, Sports, Science and Technology, Japan and a collaboration with Companhia Brasileira de Mmetallurgia e Mineração (CBMM). Lastly, this material is based upon work supported by the U.S. Department of Energy, Office of Science, Office of Basic Energy Sciences under Award Number DE-SC-0001234. The authors thank Guijun Ma at the University of Tokyo for performing the PEC measurement of Sc-$La_5Ti_2CuS_5O_7$ photoelectrodes.

## Appendix A. Supplementary material

Supplementary data associated with this article can be found, in the online version, at http://dx.doi.org/10.1016/j.cplett.2017.03.012.

## References

[1] K. Maeda, K. Domen, J. Phys. Chem. C 111 (2007) 7851–7861.
[2] J. Liu, T. Hisatomi, G. Ma, A. Iwanaga, T. Minegishi, Y. Moriya, M. Katayama, J. Kubota, K. Domen, Energy Environ. Sci. 7 (2014) 2239–2242.
[3] G. Ma, Y. Suzuki, R.B. Singh, A. Iwanaga, Y. Moriya, T. Minegishi, J. Liu, T. Hisatomi, H. Nishiyama, M. Katayama, K. Seki, A. Furube, T. Yamada, K. Domen, Chem. Sci. 6 (2015) 4513–4518.
[4] H. Urabe, T. Hisatomi, T. Minegishi, J. Kubota, K. Domen, Faraday Discuss. 176 (2014) 213–223.
[5] M. Kodera, H. Urabe, M. Katayama, T. Hisatomi, T. Minegishi, K. Domen, J. Mater. Chem. A 4 (2016) 7658–7664.
[6] L. Kronik, Y. Shapira, Surf. Interface Anal. 31 (2001) 954–965.
[7] J. Łagowski, I. Baltov, H.C. Gatos, Surf. Sci. 40 (1973) 216–226.
[8] G. Sharma, Z. Zhao, P. Sarker, B.A. Nail, J. Wang, M.N. Huda, F.E. Osterloh, J. Mater. Chem. A 4 (2016) 2936–2942.
[9] S. Li, L. Hou, L. Zhang, L. Chen, Y. Lin, D. Wang, T. Xie, J. Mater. Chem. 3 (2015) 17820–17826.
[10] J. Wang, J. Zhao, F.E. Osterloh, Energy Environ. Sci. 8 (2015) 2970–2976.
[11] J. Zhu, F. Fan, R. Chen, H. An, Z. Feng, C. Li, Angew. Chem. Int. Ed. 54 (2015) 9111–9114.
[12] T. Minegishi, N. Nishimura, J. Kubota, K. Domen, Chem. Sci. 4 (2013) 1120–1124.
[13] M.W. Kanan, D.G. Nocera, Science 321 (2008) 1072–1075.
[14] H.B. Michaelson, J. Appl. Phys. 48 (1977) 4729–4733.
[15] D.R. Lide, CRC Handbook of Chemistry and Physics, 88th ed., 2008.
[16] E. Sakai, N. Nagamura, J. Liu, T. Hisatomi, T. Yamada, K. Domen, M. Oshima, Nanoscale 8 (2016) 18893–18896.
[17] Y. Suzuki, R.B. Singh, H. Matsuzaki, A. Furube, G. Ma, T. Hisatomi, K. Domen, K. Seki, Chem. Phys. 476 (2016) 9–16.
[18] G. Ma, J. Liu, T. Hisatomi, T. Minegishi, Y. Moriya, M. Iwase, H. Nishiyama, M. Katayama, T. Yamada, K. Domen, Chem. Commun. 51 (2015) 4302–4305.
[19] R.B. Singh, H. Matsuzaki, Y. Suzuki, K. Seki, T. Minegishi, T. Hisatomi, K. Domen, A. Furube, J. Am. Chem. Soc. 136 (2014) 17324–17331.
[20] J. Zhao, F.E. Osterloh, J. Phys. Chem. Lett. 5 (2014) 782–786.
[21] D. Gal, Y. Mastai, G. Hodes, L. Kronik, J. Appl. Phys. 86 (1999) 5573–5577.
[22] Y. Ham, T. Minegishi, T. Hisatomi, K. Domen, Chem. Commun. 52 (2016) 5011–5014.